Novel *In Situ* Carbon Nanofiber/Polydimethylsiloxane Nanocomposites: Synthesis, Morphology, and Physico-Mechanical Properties

Nabarun Roy,[1] Anil K. Bhowmick[1,2]

[1]*Rubber Technology Centre, Indian Institute of Technology, Kharagpur 721302, India*
[2]*Indian Institute of Technology, Patna 800013, India*

Received 19 March 2011; accepted 6 June 2011
DOI 10.1002/app.35037
Published online 22 September 2011 in Wiley Online Library (wileyonlinelibrary.com).

ABSTRACT: A series of carbon nanofiber (CNF)/polydimethylsiloxane (PDMS)-based nanocomposites was prepared by anionic ring opening polymerization of octamethylcyclotetrasiloxane (D_4) in presence of pristine CNF and amine-modified CNF. A detailed study of morphology–property relationship of the nanocomposites was carried out in order to understand the effect of chemical modification and loading of filler on property enhancement of the nanocomposites. An elaborate comparison of structure and properties was carried out for the nanocomposites prepared by *in situ* and conventional *ex situ* methods. Pronounced improvement in degree of dispersion of the fillers in the matrix on amine modification of CNFs was reflected in mechanical properties of the modified nanocomposites. Maximum upliftment in mechanical properties was observed for *in situ* prepared amine modified CNF/hydroxyl PDMS nanocomposites. For 8 phr filler loading, tensile strength increased by 370%, while tensile modulus showed an increase of 515% compared with the virgin elastomer. Furthermore, *in situ* prepared unmodified CNF/hydroxyl PDMS nanocomposites showed an increase of 141°C in temperature of maximum degradation (T_{max}) for 8 phr CNF loading. These results were correlated with the morphological analysis through transmission electron microscopic studies. © 2011 Wiley Periodicals, Inc. J Appl Polym Sci 123: 3675–3687, 2012

Key words: polysiloxanes; carbon nanofibers; dispersions; nanocomposites; structure–property relations

INTRODUCTION

Among the one-dimensional nanoscaled carbon materials, carbon nanofibers (CNFs) are being well accepted as reinforcing additives.[1–4] In recent years, these are produced by economic techniques such as carbon ablation and chemical vapor deposition (CVD). On incorporation into polymer matrices, these result in advanced engineering high performance materials.[5,6] These are expected to improve various properties of nanocomposites due to their interfacial adhesion with polymeric phase.[7] However, CNFs show inherent tendency to form bundles due to strong lateral interactions among themselves. This causes difficulty in dispersing individual nanofibers in the matrix of a polymer and hence their outstanding properties remain untapped due to poor dispersion. Thus, proper dispersion of CNFs in a polymer matrix is the key factor in determining enhancement of properties of nanocomposites.

Homogeneous dispersion of the nanofibers in a polymer matrix can be achieved by developing strong van der Waals force of attraction between a polymer and the filler. The aim of overcoming the incompatibility between the fillers and polymer matrices and the strong tendency of self-aggregation of the nanofibers can be effectively fulfilled by chemical treatment of the filler.[7,8] Introduction of chemically attached functional groups on the surface of CNFs promotes dispersion in the polymer matrix, thereby facilitating significant energy as well as load transfer across the interface and hence improving the mechanical properties of the nanocomposites.[9,10] *In situ* preparation of nanocomposites facilitates good dispersion of fillers in a polymer matrix.[11,12] This technology has been explored in the recent years to affect significant dispersion of nanofillers in polymer matrix.

Because of their promising mechanical strength, CNFs are effective in upliftment of mechanical properties of the nanocomposites. Various thermoplastic and thermosetting polymers such as polypropylene (PP),[13–18] polycarbonate,[19–21] poly(ether ether ketone),[22] nylon,[23] epoxy,[24] etc., have been used in nanocomposite preparation. However, no work has been reported till date on CNF/PDMS nanocomposites.

PDMS exhibits a bouquet of exquisite properties owing to its unique structural features. Its high

Correspondence to: A. K. Bhowmick (anilkb@rtc.iitkgp.ernet.in or director@iitp.ac.in).

Contract grant sponsors: Council of Scientific and Industrial Research (CSIR), New Delhi.

thermal stability, low temperature flexibility, biocompatibility, good air permeability widens its gamut of applications.[25–28] However, its poor mechanical strength limits its application in those cases where strength is a critical concern. Thus, an attempt can be made to prepare nanocomposites by exploring the excellent mechanical properties of CNF. Nanocomposite preparation with these two materials is challenging due to a huge surface energy difference between the two phases. This may lead to improper dispersion of the fibrous phase in the matrix. Furthermore, it is a well agreed fact that chemical modification improves dispersion of nanofibers in a polymer matrix leading to improvement in various physico-mechanical properties. Thus, in this study, an attempt has been made to improve dispersion of filler in the polymer matrix by *in situ* synthesis of nanocomposites. Additionally, chemical modification of filler was carried out in order to get an insight into the influence of filler modification and *in situ* nanocomposite preparation on the dispersion state of the filler and hence on the physico-mechanical properties of the nanocomposites.

Literature review reveals that work based on CNF/PDMS nanocomposites is very scanty. The plausible reason for this is the improper dispersion of the CNFs in the polymer matrix. Thus in this work, for the first time CNF/PDMS nanocomposites have been prepared by anionic ring opening polymerization of octamethylcyclotetrasiloxane (D_4) in presence of CNF. Amine modification of CNF has been carried out and *in situ* nanocomposites have been prepared with the same. The nanocomposites prepared have been characterized by Transmission Electron Microscopy (TEM), Attenuated Total Reflection-Fourier Transform Infrared Spectroscopy (ATR-FTIR), swelling studies, mechanical and thermal properties measurements. The results obtained have been compared with those of the nanocomposites prepared by conventional *ex situ* method.

EXPERIMENTAL

Materials

Octamethylcyclotetrasiloxane $[(CH_3)_2SiO]_4$ (D_4), Platinum catalyst (Pt catalyst in U-10, where U-10 is a vinyl PDMS system having a molecular weight 74,400 and viscosity 10 Pa s) and the hydride crosslinker polymethylhydrogenosiloxane (V430) with the chemical formula $Me_3Si(OSiMe_2)_x(OSiMeH)_yOSiMe_3$, where x and y are 10, having hydride content of 4.3 mmol/g were provided by Momentive Performance Materials, Bangalore, India. The monomer D_4 with a boiling point of 175°C having purity > 99% (GC) was freshly distilled before use.

1, 1, 3, 3-Tetramethyl-1, 3-divinyldisiloxane with purity 97% having a boiling point 139°C was purchased from Sigma-Aldrich, USA.

Potassium hydroxide was procured from Merck, Mumbai, India.

CNFs (as grown grade PR-24 AG Pyrograf-III) were obtained from Applied Sciences, USA. The CNF consists of relatively straight cylindrical tubes.

Tetraethoxysilane (TEOS) was obtained from Acros Organics, NJ, USA.

Dibutyltin dilaurate (DBTDL) was procured from Aldrich Chemicals, Bangalore, India.

Hexamethylenediamine (HMDA) or 1, 6-Diaminohexane was procured from Merck, Merck Schuchardt OHG, Germany.

Synthesis of pristine PDMS- and PDMS-based nanocomposites

Surface functionalization of CNFs

The amination was done by treating 3 g of nanofibers with excess of HMDA within a 250-mL three-necked round-bottomed flask at 130 ± 10°C in an oil bath for 24 h. The modified nanofibers were then washed with alcohol to remove the excess of amine present. This was followed by washing with distilled water to remove the alcohol. The nanofibers were then subjected to filtration using nylon membrane filter paper of 0.45 μm pore size followed by vacuum drying at 80°C. This procedure is similar to that developed previously by George and Bhowmick.[29]

Synthesis of vinyl terminated PDMS-based nanocomposites

In situ vinyl terminated PDMS-based nanocomposites were prepared following the procedure adopted in our previous publication.[12] Briefly, 15 g of D_4 and 0.08 g of KOH were reacted at 140°C under nitrogen atmosphere in presence of nanofiller for 2 h followed by addition of 1, 1, 3, 3-Tetramethyl-1, 3-divinyldisiloxane. The reaction was terminated after 4 h and was left overnight.

Work up and curing of nanocomposites

The nanocomposite was soaked in toluene and unreacted base was neutralized by H_3PO_4. This was followed by addition of platinum catalyst and Si-H crosslinker to the resulting solution which was then cast in a teflon petridish for curing. On solvent evaporation, cured sheet of PDMS composite was obtained.

Synthesis of hydroxyl-terminated PDMS

Totally, 15 g (0.05 mole) of octamethylcyclotetrasiloxane (D_4) was distilled in the similar way as for vinyl

TABLE I
Sample Preparation Along with Their Designations

Sample	D_4 used (g)	KOH (g)	Vinyl terminator (g)	Polymer obtained (g)	Amount of Si-H crosslinker (g)	Amount of TEOS (g)	Amount of CNF (with respect to the polymer obtained) (phr)
VP C0	15	0.08	0.05	13	0.32	–	–
VP C1	15	0.08	0.05	13	0.32	–	1
VP C2	15	0.08	0.05	13	0.32	–	2
VP C4	15	0.08	0.05	13	0.32	–	4
VP C8	15	0.08	0.05	13	0.32	–	8
VP C2A	15	0.08	0.05	13	0.32	–	2
VP C4A	15	0.08	0.05	13	0.32	–	4
VP C8A	15	0.08	0.05	13	0.32	–	8
VP C4E[a]	15	0.08	0.05	13	0.32	–	4
VP C8E[a]	15	0.08	0.05	13	0.32	–	8
PD C0	15	0.08	–	13	–	0.5	–
PD C1	15	0.08	–	13	–	0.5	1
PD C2	15	0.08	–	13	–	0.5	2
PD C4	15	0.08	–	13	–	0.5	4
PD C8	15	0.08	–	13	–	0.5	8
PD C10	15	0.08	–	13	–	0.5	10
PD C1A	15	0.08	–	13	–	0.5	1
PD C2A	15	0.08	–	13	–	0.5	2
PD C4A	15	0.08	–	13	–	0.5	4
PD C8A	15	0.08	–	13	–	0.5	8
PD C10A	15	0.08	–	13	–	0.5	10
PD C4E[a]	15	0.08	–	13	–	0.5	4
PD C8E[a]	15	0.08	–	13	–	0.5	8

VP, PD, and C stand for vinyl PDMS, hydroxyl PDMS and carbon nanofiber respectively.
A signifies amine modified carbon nanofiber filled nanocomposites.
[a] Stands for the samples prepared by *ex situ* method.

terminated PDMS. 0.08g (0.5%) of KOH was finely grinded in nitrogen atmosphere and was introduced into the flask. The reaction was continued for two hours at 140°C. Polymerization was evidenced by rise in viscosity of the resultant mixture. This was left undisturbed overnight before the workup.

Work up of the hydroxyl terminated PDMS

Work up of the synthesized PDMS was done in exactly the same way as that with vinyl terminated PDMS.

Curing of hydroxyl terminated PDMS

Thirteen grams of the polymer obtained was dissolved in 20 mL of toluene to make a homogeneous solution. To this 0.5 g of TEOS was added and the resulting mixture was stirred using a magnetic stirrer for a few minutes. This was followed by the addition of 0.025 g of DBTDL and a constant stirring for a minute. The final mixture was degassed for 10 minutes to remove unwanted gaseous volatiles and was cast in a Teflon petridish and left undisturbed overnight. This resulted in a transparent sheet of $\sim$ 0.5 mm thickness which was ultimately vacuum-dried at 80°C.

Synthesis of hydroxyl-terminated PDMS-based nanocomposites

Varying amounts of modified and unmodified CNF was soaked in D_4 and left overnight. The monomer containing CNF was sonicated for 10 min in order to deagglomerate the filler in the monomer phase. This was followed by addition of same amount of base and the reaction was carried out in the same way as with pristine PDMS. Even work up and curing was done following the same procedure and using same amount of reagents.

Synthesis of *ex situ* CNF/PDMS nanocomposites by solution casting

Vinyl PDMS and hydroxyl PDMS were synthesized by same polymerization technique as mentioned earlier. Calculated amount of CNF was dispersed in toluene and sonicated for 15 min. This was then added to the polymer solution and stirred for 2 h. To the resulting solution, curing agent was added, the mixture was degassed, cast in Teflon petridish and left overnight for curing at room temperature. The samples along with their compositions and designations are compiled in Table I.

Instrumentation

Characterization of synthesized PDMS

Number average molecular weight. To determine number average molecular weight of the synthesized PDMS ^{29}Si Nuclear Magnetic Resonance (NMR) spectra of pristine vinyl endcapped PDMS and hydroxyl PDMS were taken using Bruker AM-360, 400 MHz NMR spectrometer with tetramethylsilane (TMS) as the internal standard and a paramagnetic relaxation agent such as chromium acetylacetonate for exact integration. The concentrations of samples in $CDCl_3$ solution were 50 % w/v. For acquiring ^{29}Si NMR spectra a heteronuclear gated decoupled pulse sequence (NONOE) was used.

Characterization of nanocomposites

Transmission electron microscopy. The samples for transmission electron microscopy (TEM) analysis were prepared by ultra-cryomicrotomy with a Leica Ultracut UCT (Leica Microsystems GmdH, Vienna, Austria). Freshly sharpened glass knives with cutting edges of 45° were used to obtain cryosections of about 100–150 nm thickness at −150°C. The cross sections were collected individually in sucrose solution and directly supported on a copper grid of 300 mesh. Microscopy was performed with JEOL 2100, Japan. Transmission electron microscope was operated at an accelerating voltage of 200 kV.

Attenuated total reflection-Fourier transmission infrared (ATR-FTIR) spectroscopy. An infrared spectrophotometer (Nicolet Nexus, Madison, WI) was used to acquire the Attenuated total reflection (ATR)-Fourier transmission infrared (FTIR) spectra of the samples within a range of 650 cm^{-1} to 4000 cm^{-1} taking a resolution of 4 cm^{-1} using a ZnSe prism. An average of 120 scans was accounted for each spectrum.

Swelling analysis. The swelling studies of the rubber specimens have been carried out in toluene at ambient conditions (27°C) for three days. The volume fraction of rubber in swollen gel (V_r) is calculated using eq (1).[30]

$$V_r = \frac{(D_s - F_f A_w)\rho_r^{-1}}{(D_s - F_f A_w)\rho_r^{-1} + A_s \rho_s^{-1}} \quad (1)$$

where,

A_w = weight of test specimen.

D_s = deswollen weight of the test specimen.

F_f = weight fraction of insoluble components.

A_s = weight of absorbed solvent corrected for swelling increment.

ρ_r = density of rubber.

ρ_s = density of the solvent

The apparent crosslink density was calculated according to Flory-Rehner[31] equation using the value of V_r as follows [eq. (2)].

$$-[\ln(1 - V_r) + V_r + \chi V_r^2] = \frac{\rho_r}{M_c} \times V_s \left(V_r^{1/3} - \frac{V_r}{2} \right) \quad (2)$$

where,

χ = Flory–Huggins polymer–solvent interaction parameter

ρ_r = density of rubber

M_c = molecular weight between crosslinks

V_s = molar volume of the solvent

The results shown were mean values of three experiments performed for each sample. The mean error of the measurement was ±3% for the above measurements.

where, χ is Flory–Huggins-interaction parameter. Its value is 0.465 for PDMS–toluene system. V_r is the volume fraction of rubber in the swollen gel, F_f the fraction insoluble, D_s the deswollen weight of the nanocomposites, A_w the initial weight of the sample, and A_s the amount of solvent imbibed. ρ_r is the density of the rubber and ρ_r is density of the swelling solvent.

Thermogravimetric analysis. The thermogravimetric analysis (TGA) analysis was carried out with 3–5 mg sample in Perkin Elmer Instrument, Diamond TG-DTA, at the heating rate of 20°C/min under air atmosphere up to 800°C. The data was analyzed by TA Universal analysis software. The temperature at which maximum degradation takes place has been denoted by T_{max} and onset temperature of degradation has been denoted by T_i. The error in the measurement is ± 1°C.

Mechanical properties. Dumb-bell shaped samples (tensile specimens) ASTM D 412-98 were punched out from the solution cast sheets using ASTM Die-C. The tensile tests were performed on a Zwick UTM, Model – Z010 (Zwick GmbH and Co., Ulm, Germany) at a cross-head speed of 500 mm/min at 25°C. The average of three tests is reported here.

Dynamic mechanical analysis. The dynamic mechanical data of the samples (12.59 mm × 6.65 mm × 1.2 mm) were obtained by using a dynamic mechanical analysis (DMA) of TA instruments (model Q800). The sample specimens were analyzed in tensile mode at a constant frequency of 1 Hz, a strain of 0.05% and a temperature range from –130 to 50°C at a heating rate of 2°C/min. The data were analyzed by TA Universal analysis software on a TA computer attached to the machine. Loss tangent (tan δ) was measured as a function of temperature for all the samples under identical conditions. The temperature corresponding to the peak in tan δ versus temperature plot was taken as the glass-rubber transition temperature (T_g).

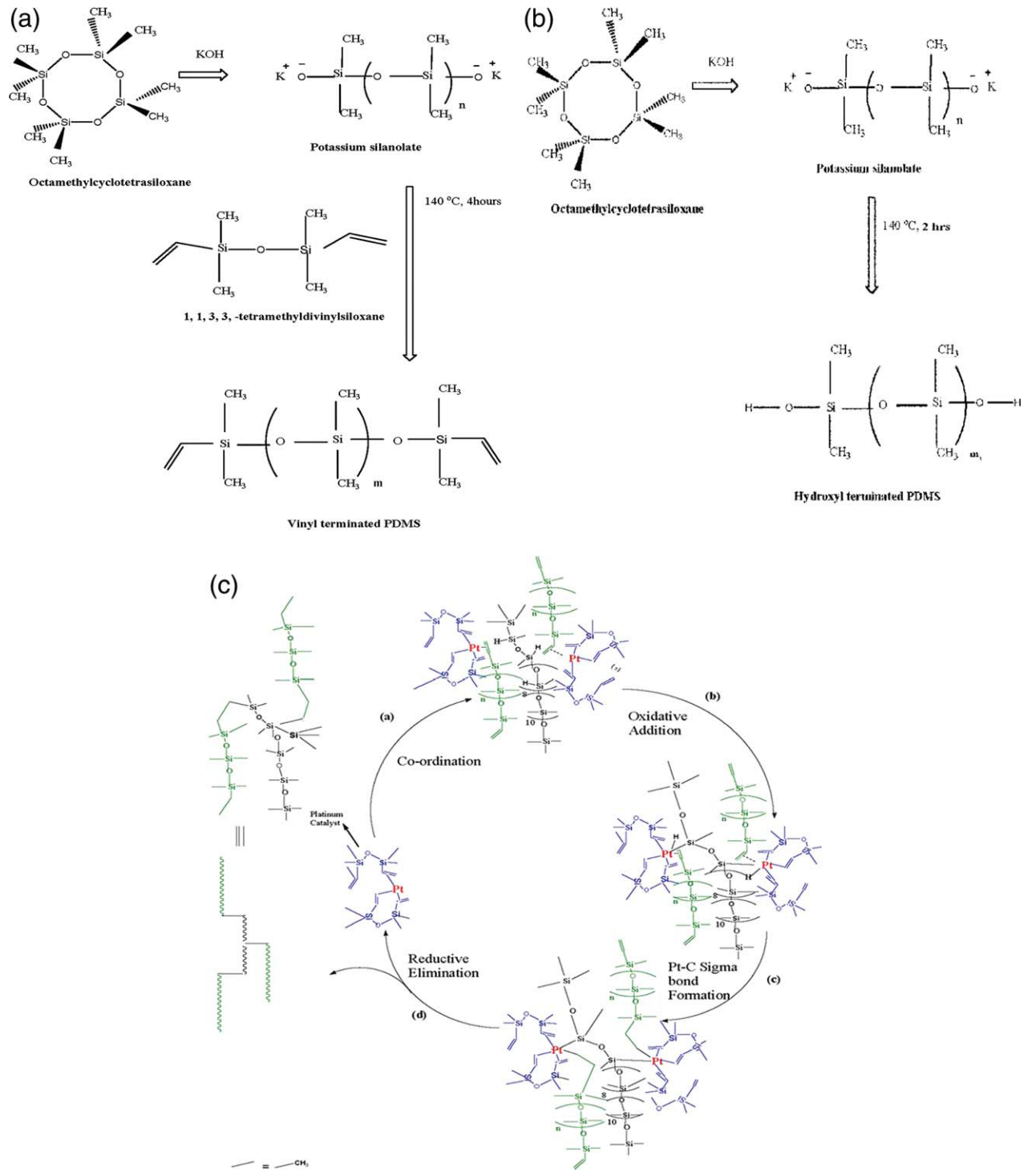

Figure 1 (a) Scheme of the polymerization reaction for vinyl endcapped PDMS. (b) Scheme of the polymerization reaction for hydroxyl PDMS. (c) Platinum catalyzed hydrosilylation of vinyl PDMS. [Color figure can be viewed in the online issue, which is available at wileyonlinelibrary.com.]

RESULTS AND DISCUSSION

Synthesis of vinyl and hydroxyl terminated PDMS and curing reaction

Synthesis of vinyl and hydroxyl PDMS has been carried out by anionic ring opening polymerization of D_4.[32] The reaction scheme is shown in Figure 1(a,b), respectively. Curing of vinyl PDMS is based on platinum catalyzed hydrosilylation reaction[33] as shown in Figure 1(c). Curing of the hydroxyl functional PDMS has been done with TEOS and DBTDL following the principle of hydrolysis and condensation.

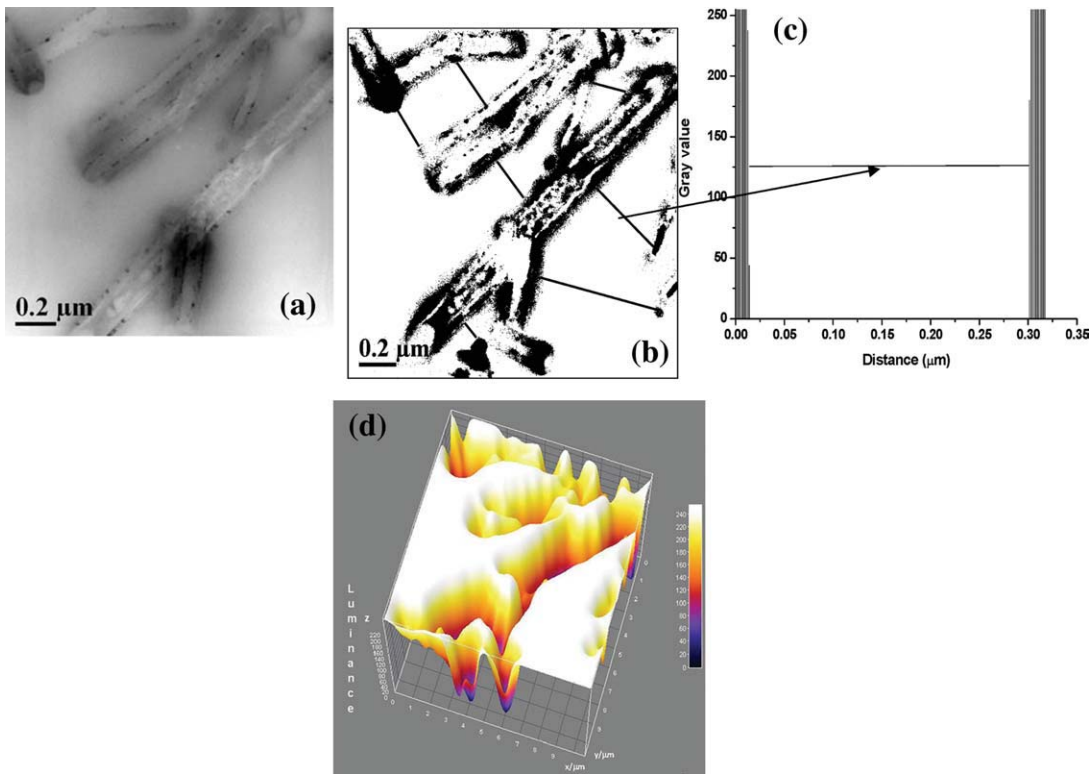

Figure 2 (a) TEM image (b) thresholded image of 4 phr CNF filled vinyl endcapped PDMS nanocomposite (c) Plot of gray value versus distance. (d) 3D interactive plot profile of *in situ* prepared CNF(4 phr)/vinyl PDMS nanocomposite. [Color figure can be viewed in the online issue, which is available at wileyonlinelibrary.com.]

TEM studies

TEM studies give a clear picture for the dispersion state of the nanofibers in the PDMS matrix. Quantification of the dispersion degree has been done by introducing the dispersion degree parameter $D_{0.1}$, which is defined as the free path distance distribution and lies in the range of 0.9 $\overline{x}$ to 1.1 $\overline{x}$, where $\overline{x}$ is the mean spacing between the nanofibers. Higher the value of $D_{0.1}$, better is the dispersion. Free path distribution follows a lognormal distribution model[34] and $D_{0.1}$ is formulated as:

$$D_{0.1} = 1.1539 \times 10^{-2} + 7.5933 \times 10^{-2}(\overline{x}/s) + 6.6838 \times 10^{-4}(\overline{x}/s)^2 - 1.9169 \times 10^{-4}(\overline{x}/s)^3 + 3.9201 \times 10^{-6}(\overline{x}/s)^4 \quad (3)$$

where s is the standard deviation.

Based on the free path data, mean and standard deviation are obtained using the expressions $\overline{x} = \sum_i \frac{x_i}{N}$ and $s = \sqrt{\frac{\sum_i (x_i - \overline{x})^2}{(N-1)}}$ respectively. The ratio $\frac{\overline{x}}{s}$ is used to calculate $D_{0.1}$.

Figure 2(a) shows the TEM image of *in situ* prepared 4 phr CNF loaded vinyl PDMS nanocomposite. To determine the dispersion state of the nanofibers the TEM image is processed using Image J software. In order to remove uneven illumination, background subtraction is done. This is followed by smoothening of the image to remove noise if any and conversion into threshold image shown in Figure 2(b).

Free path is determined by using randomly a line tool shown in Figure 2(b) and consecutively constructing the plot profile of the selective scanned region as shown in Figure 2(c). The distance with zero gray value corresponds to the matrix region separating two individual fibers and is a measure of the free path.

Figure 2(d) shows a plot of luminance versus the area scanned. The most illuminated area (matrix of the polymer) is raised high while the fibers are embedded low in the plot. Thus this interactive 3D plot gives an idea of the three-dimensional form of the TEM image.

Several measurements ($N = 260$) in terms of free path are done as mentioned and a histogram is constructed. A lognormal fit is imposed on it and $\frac{\overline{x}}{s}$ is used to determine $D_{0.1}$.

Figure 3 shows the histogram for free path distribution data for *in situ* prepared unmodified CNF/PDMS (4 phr) nanocomposite. From the lognormal fit, the mean spacing and standard deviation are

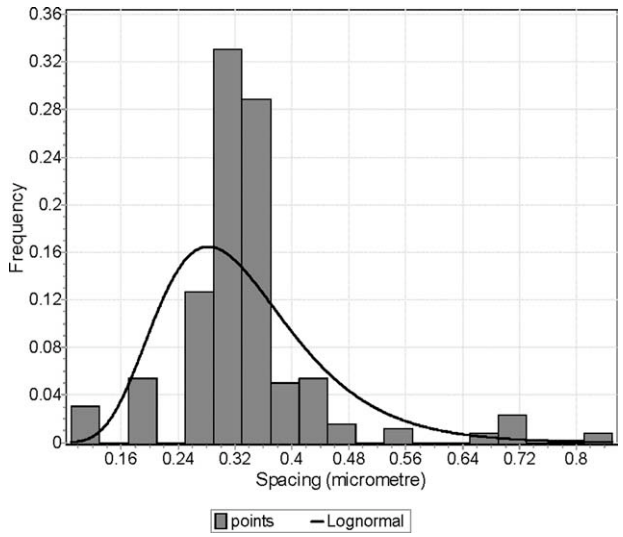

Figure 3 Representative plot of frequency versus distance between the nanofibers for *in situ* CNF/vinyl endcapped PDMS (4 phr) nanocomposite.

calculated to be $\overline{x} = 0.33$ μm and $s = 0.106$ μm respectively which gives $\overline{x}/s = 3.113$. This results in a $D_{0.1}$ value of 24.87%.

Effect of nanocomposite preparation on dispersion of nanofillers

A comparative study of the dispersion degree is made in order to understand the state of dispersion of nanofibers for *in situ* prepared nanocomposites with those prepared by conventional *ex situ* method. TEM images of *ex situ* prepared nanocomposites feature prominent agglomeration of nanofibers in the form of lumps. Figure 4(a) is a representative TEM image of 4 phr unmodified CNF loaded *ex situ* nanocomposite. The mean spacing in this case is found to be $\overline{x} = 0.104$ μm with a standard deviation $s = 0.079$ μm which results in $\overline{x}/s = 1.328$. Thus, a very low value of $D_{0.1}$ (11.69%) is observed for these nanocomposites.

Effect of chemical modification of nanofillers on state of dispersion

Functionalization of fillers results in notable improvement in dispersion of the fillers in the polymer matrices.[35] In a similar way, in this case amine modification of CNFs significantly improves the extent of dispersion of the individual fibers in the matrix and thereby improves various physico-mechanical properties of the nanocomposites as discussed later. High degree of dispersion of the individual nanofibers is evident from Figure 4(b) which is much better than *ex situ* as well as *in situ* prepared nanocomposites with unmodified CNF. In this case, from the histogram shown in Figure 5, $\overline{x}$ and s are calculated to be 0.34 and 0.084 μm, respectively. From these values $\overline{x}/s = 4.047$ which gives a much higher $D_{0.1}$ value of 31.81%. The probable factor for this higher value of $D_{0.1}$ is the H-bonding interaction between the amine groups on the filler surface and PDMS backbone which facilitates intimate polymer–filler interaction.

ATR-FTIR analysis

Figure 6 shows the ATR-FTIR spectra of virgin vinyl PDMS and its nanocomposites with unmodified and amine modified CNF at same filler loading. FTIR spectrum of PDMS shows characteristic absorptions for the following structural features: prominent peaks are found at 2964 cm^{-1} for asymmetric CH stretch, 1408 cm^{-1} due to CH_3 asymmetric deformation, 1259 cm^{-1} CH_3 symmetric deformation, Si—O—Si asymmetric deformation around 1020 cm^{-1}, Si—O—Si skeletal stretching at 790 cm^{-1} and 695 cm^{-1} for the surface.[36]

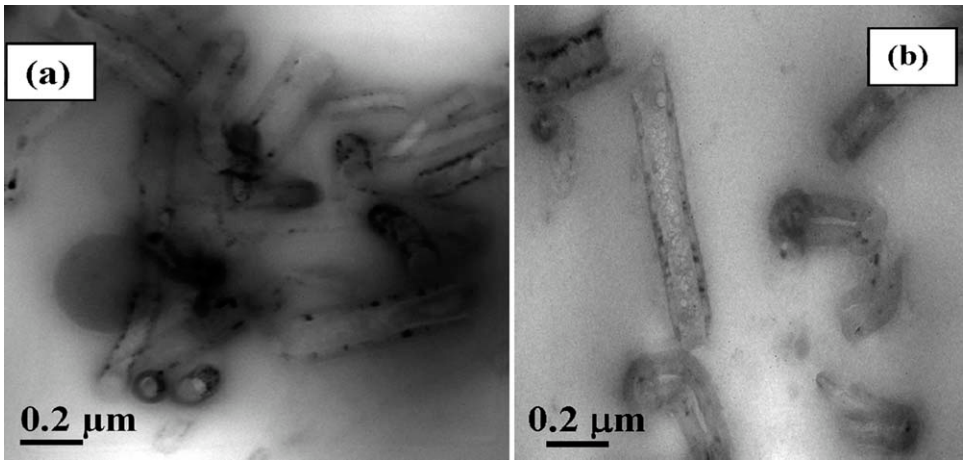

Figure 4 TEM image of (a) *ex situ* prepared unmodified CNF/vinyl PDMS nanocomposite (4 phr) (b) *in situ* prepared amine-modified CNF/vinyl PDMS nanocomposite (4 phr).

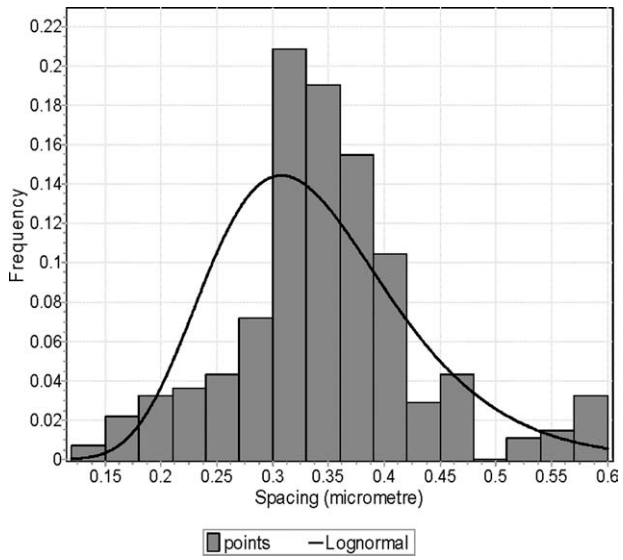

Figure 5 Representative plot of frequency versus distance between the nanofibers for *in situ* vinyl endcapped amine modified CNF/vinyl PDMS (4 phr) nanocomposite.

For amine modified CNF-based nanocomposites, shift in absorption for Si—O—Si asymmetric stretch is observed. This may be due to the fact that the amine functionalities on the CNF surface interact with the O atom in the main polymer backbone through H-bonding. But in the case of unmodified CNF-based nanocomposites, almost no change in the position of this peak is observed as functional groups are absent in this case. Moreover, the presence of amine functionalities is well observable for the nanocomposite with amine modified CNF from the peak around 3500 cm^{-1} which is due to the N—H group. This confirms the presence of $—NH_2$ groups on the filler which can participate in H-bonding interaction with the O atom of the Si—O backbone. Furthermore, the intensity of this peak gradually increases with increase in filler concentration as evident from the inset of Figure 6. A schematic representation of the H-bonding between the amine groups on the filler surface and the O atom in the PDMS backbone has been made in Figure 7.

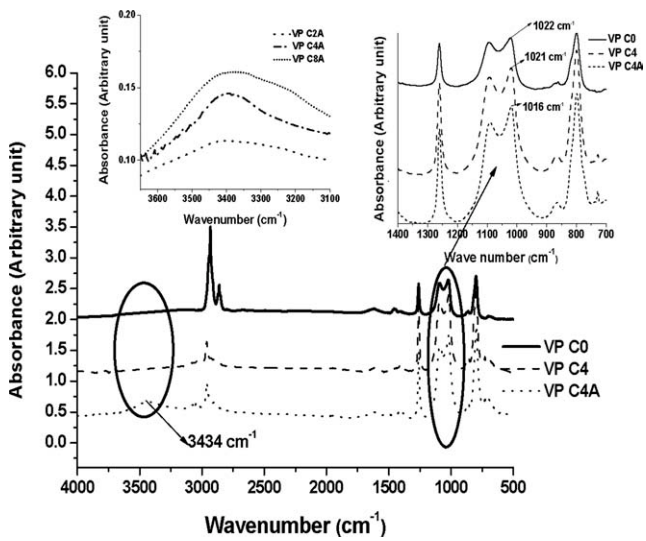

Figure 6 Comparison of the FTIR plots of unfilled, unmodified, and amine modified CNF-filled vinyl PDMS systems.

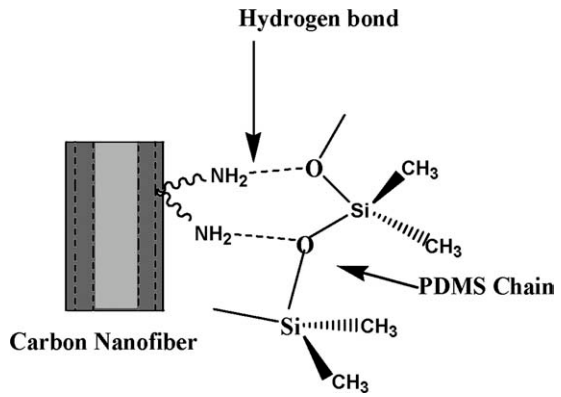

Figure 7 Schematic representation of H-bonding between the amine functionalities of the filler modifier and the PDMS backbone.

Swelling studies

Figure 8 shows the plots of crosslink density for unmodified and amine-modified CNF-based nanocomposites for hydroxyl PDMS systems. *In situ* prepared nanocomposites show higher crosslink density compared with *ex situ* prepared nanocomposites. This is reflected in the properties discussed later. Besides nonbonding forces of attraction commonly responsible for upliftment of CNF-based nanocomposites, PDMS-amine modified CNF nanocomposites show H-bonding interaction between the O atom in the PDMS main backbone and the N—H functionalities of the amine groups on the filler surface. This

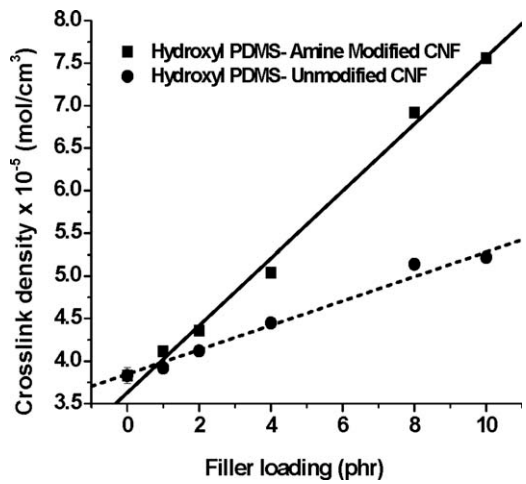

Figure 8 Comparison of crosslink densities of the neat polymer and CNF filled hydroxyl PDMS-based nanocomposites.

TABLE II
Comparison of Crosslink Density of Various Nanocomposites at Same Filler Loading

Sample	Crosslink density $\times 10^{-5}$ mol/cm^3
VP C4	4.25 ± 0.06
VP C4A	2.67 ± 0.02
VP C4E	4.07 ± 0.12
PD C4	4.45 ± 0.03
PD C4A	5.04 ± 0.05

additional interaction is expected to impart enhanced interaction between the two phases and increase crosslink density since these H-bonded sites act as physical crosslinks.

However, it is found that for vinyl terminated PDMS-based nanocomposites, there is a decrease in crosslink density for the amine modified CNF-based nanocomposites as compared with the unmodified CNF-based systems for the same filler concentration. This is evident from the results compiled in Table II.

Detailed studies with the curing systems for vinyl PDMS revealed that Si—H bonds are very much susceptible to amines (Lewis bases) leading to liberation of hydrogen.[37] Thus, it may be concluded that presence of amine groups on the fiber surface consumes the reactive Si—H groups of the crosslinker thereby decreasing the effective amount of the latter. The extent of this side reaction increases with increase in the amount of the filler. Polymer–filler interaction, on the other hand, increases with increase in filler content. The extent of interaction is also influenced by filler agglomeration at higher concentrations. Thus, these factors lead to a decrease in crosslink density of the amine modified CNF-based nanocomposites. The effect of decrease in crosslink density is reflected in the various properties of the nanocomposites in the subsequent sections.

With hydroxyl terminated PDMS as the matrix, crosslink density of the amine modified PDMS-based nanocomposites is higher compared with the unmodified CNF-based system at same filler loading. Since, here the crosslinking system (TEOS in presence of DBTDL) is unaffected by the amine functionalities, the effect of the filler in increasing the interfacial adhesion through H-bonding interaction is quite evident. Increased crosslink density suggests strong interface formation between polymer and filler.[38] This is the consequence of better dispersion of the filler in polymer matrix.

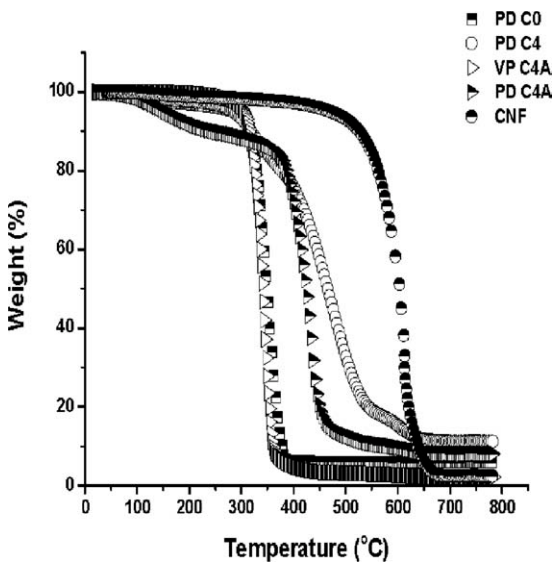

Figure 9 Representative TGA plots of CNF and CNF/PDMS nanocomposites.

Thermogravimetric studies

Figure 9 shows a comparative plot of thermograms of pristine PDMS and its nanocomposites with unmodified and amine modified CNF and the results of the TG analysis have been compiled in Table III. The nature of the plots for temperature dependence of the nanocomposites is usually sigmoid. From the figure, it is observed that thermal degradation of the nanocomposites shifts to higher temperature with increasing loading of filler. This substantiates formation of a polymer–filler interface which is the consequence of interaction between the macromolecular chains and the filler.

Thermal stability of unmodified CNF-based nanocomposites

For vinyl PDMS system with unmodified CNF, T_{max} increases by 11, 42, 100, and 138°C for 1, 2, 4, and 8 phr of filler loadings respectively, while temperature

TABLE III
Results of Thermogravimetric Analysis of Unfilled and CNF-Filled PDMS Vulcanizates

Sample	T_{max} (°C)	T_i (°C)	Ash content (%)
VP C0	350	332	18
VP C1	361	339	22
VP C2	392	344	24
VP C4	450	376	27
VP C8	488	424	32
VP C4E	403	366	21
PD C0	341	316	6
PD C1	355	335	11
PD C2	386	370	13
PD C4	435	402	16
PD C8	482	414	21
PD C1A	363	337	7
PD C2A	399	378	8
PD C4A	425	399	11
PD C8A	455	429	16
PD C10A	461	421	17

of initiation of degradation (T_i) increases by 7, 12, 44, and 92°C in the same sequence.

For *in situ* prepared unmodified CNF/hydroxyl terminated PDMS nanocomposites, T_{max} shows an increment of 14, 45, 94, and 141°C, while T_i increases by 19, 54, 86, and 98°C respectively for 1, 2, 4, and 8 phr loadings of filler. It is by the virtue of the *in situ* method of nanocomposite preparation which results in lesser extent of agglomeration of the CNFs as observed in TEM studies. However, quite interestingly CNF in the nanocomposites decomposed at a lower temperature compared to the pristine CNF as observed by Xu et al.[39] It is established that the ash content in oxidative thermal degradation of PDMS yields silicon carbide or oxycarbide as one of the components besides silica.[40] For the nanocomposites, ash content is found to increase with increasing filler content. This is probably due to the fact that the nanofibers react at high temperature with the depolymerizing PDMS to produce silicon carbide and oxycarbide. The amount of this material goes on increasing with increasing concentration of filler in the nanocomposite. In case of the nanocomposites, the thermally stable filler particles restrict oxygen from depolymerizing PDMS by barrier mechanism and hence reduce the rate of degradation reaction. The competitive oxidative crosslinking stabilizes the product thereby increasing the ash content nonstoichiometrically.

Effect of method of preparation

Ex situ prepared nanocomposites do not show improved thermal stability to the extent shown by i*n situ* prepared nanocomposites. While for VP C4, T_{max} and T_i are respectively 450 and 376°C, these are respectively just 403 and 366°C for VP C4E (*ex situ*). This is most probably due to poor dispersion of the filler in the polymer matrix as has been observed from image analysis of TEM micrographs.

Effect of amine modification of filler

There is no observable change in T_{max} and T_i when compared with those of virgin rubber with increasing filler loading for amine modified CNF-based vinyl PDMS systems. This is observed for amine modified CNF/vinyl PDMS-based system only. In fact, both these parameters undergo no prominent change for these systems in comparison to the unfilled system. The probable reason for this is side reaction between the Si—H crosslinker and the amine groups which adversely affects the thermal stability of the nanocomposites. This is evident from the crosslink density measurements.

Comparison of the thermal stability of amine-modified CNF-based nanocomposites with virgin hydroxyl terminated PDMS suggests that there is a prominent shift in the T_i and T_{max} values towards higher temperature side. For amine modified CNF/hydroxyl PDMS-based systems, T_{max} shows an increase of 22, 58, 84, 114, and 120°C for 1, 2, 4, 8, and 10 phr of filler loadings, while increase in T_i occurs by 21, 62, 83, 113, and 105°C for the same filler loadings respectively. The overall oxidative stability of the amine modified nanocomposites is less compared with unmodified CNF-filled systems of the same loadings, especially at higher loadings, though it is much higher compared with the virgin elastomer. This may be due to the fact that the amino groups introduced on the filler surface create a basic environment and hence catalyze the PDMS decomposition reaction. This happens since it is established that decomposition of PDMS is catalyzed by lewis base.[41]

Mechanical properties

Effect of method of preparation

Tensile tests performed on the samples show the reinforcing effect of CNF on the PDMS matrix. Mechanical properties are the outcome of several factors: aspect ratio of filler, degree of dispersion, and matrix-filler adhesion to form a strong interface.[42,43] It is found that tensile strength and tensile modulus increase with increase in filler concentration in the matrix for all the systems. This is due to the fact that with increase in filler concentration, number of physical crosslinks between filler and polymer, in terms of nonbonding forces of attraction, increases.[41] This is evident from the crosslink density measurement as discussed in one of the earlier sections. However, the extent of increase in these parameters is not the same for various systems. Improvement is much more prominent for *in situ* prepared unmodified CNF/vinyl PDMS nanocomposites compared to those prepared by conventional *ex situ* method (in this case solution casting). Tensile strength increases by 75, 99, 109, and 150% for 1, 2, 4, and 8 phr respectively, while modulus increases by 151, 176, 184, and 310 % for *in situ* prepared unmodified CNF/vinyl PDMS nanocomposites. However, the increase in tensile strength for *ex situ* prepared nanocomposites is found to be just 89 and 97 % for 4 and 8 phr CNF respectively. This is probably due to varying state of dispersion of the nanofibers in the elastomeric matrix as evident from TEM studies.

Figure 10 shows the % improvement in various parameters related to mechanical properties such as tensile strength, tensile modulus, and modulus at 100% elongation with respect to the method of preparation (*in situ* versus *ex situ*). The results compiled in the plot shows that the method of preparation of

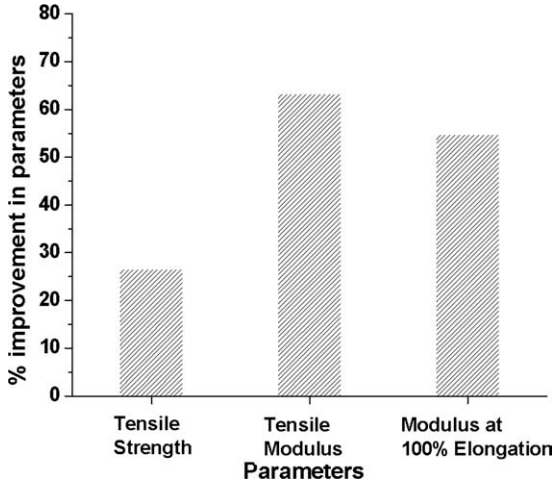

Figure 10 Plot of percentage improvement in various parameters for *in situ* prepared vinyl PDMS nanocomposites in comparison to conventional *ex situ* prepared nanocomposites at 8 phr filler loading.

the nanocomposites has a tremendous impact upon various properties owing to the difference in the degree of filler dispersion.

Effect of amine modification of CNF on the mechanical properties of vinyl PDMS-based nanocomposites

For *in situ* prepared amine modified CNF-vinyl PDMS nanocomposites, mechanical properties show minimal improvement with increase in filler loading. Increase in tensile strength is only 45 and 54% for 1 and 2 phr of filler loading, respectively. For higher loadings improper curing leads to deterioration of properties due to side reaction between functional groups on filler and reactive groups of the cross-linker. Several factors such as polymer–filler interaction, filler agglomeration at higher concentration, and the side reaction contribute to a minor improvement in mechanical strength. As a consequence, the objective of improving the mechanical properties of the nanocomposites is not effectively fulfilled.

TABLE IV
Comparison of the Mechanical Properties of Neat Rubber Vulcanizate and Its Nanocomposites

Sample	E_{mod} (kPa)	Tensile strength (TS) (kPa)	Elongation at break (EAB) (%)
VP C0	140 ± 20	167 ± 12	506 ± 59
VP C1	352 ± 10	292 ± 11	145 ± 6
VP C2	387 ± 21	333 ± 16	120 ± 4
VP C4	398 ± 11	349 ± 4	124 ± 7
VP C8	575 ± 23	418 ± 12	105 ± 1
VP C2A	352 ± 13	243 ± 8	154 ± 3
VP C4A	553 ± 4	258 ± 13	129 ± 11
VP C4E	177 ± 12	317 ± 11	210 ± 15
VP C8E	352 ± 21	330 ± 7	177 ± 18
PD C0	283 ± 21	238 ± 12	208 ± 6
PD C1	316 ± 15	254 ± 3	196 ± 9
PD C2	377 ± 11	292 ± 11	182 ± 3
PD C4	487 ± 15	439 ± 7	129 ± 6
PD C8	580 ± 25	553 ± 14	100 ± 9
PD C1A	420 ± 11	346 ± 7	227 ± 13
PD C2A	538 ± 7	458 ± 13	181 ± 6
PD C4A	915 ± 22	566 ± 22	170 ± 4
PD C8A	1740 ± 18	1120 ± 25	155 ± 3

Effect of change in matrix system to hydroxyl terminated PDMS

A switch over to the functionally different matrix system results in overwhelming increase in tensile strength and modulus as observed from Table IV. Tensile strength for *in situ* prepared unmodified CNF hydroxyl PDMS-based nanocomposites increases by 7, 23, 84, and 132 % for 1, 2, 4, and 8 phr filler loading while tensile modulus increases by 12, 33, 72, and 105% for 1, 2, 4, and 8 phr of unmodified CNF. Thus, increased polymer–filler interaction and also the penetration of the polymer molecules into the cylindrical hollow core of the nanofibers as facilitated by the lubricating graphitic systems at high reaction temperature is manifested in the improved mechanical properties for the latter.[44] Elongation at break (EAB) shows a rather irregular trend although there is a net decrease for the nanocomposites due to restricted macromolecular mobility.[45] This is also an evidence for the polymer–filler interaction leading to enhanced interface adhesion. Table IV is the compilation of the mechanical properties measurements for the neat rubber vulcanizate and its nanocomposites.

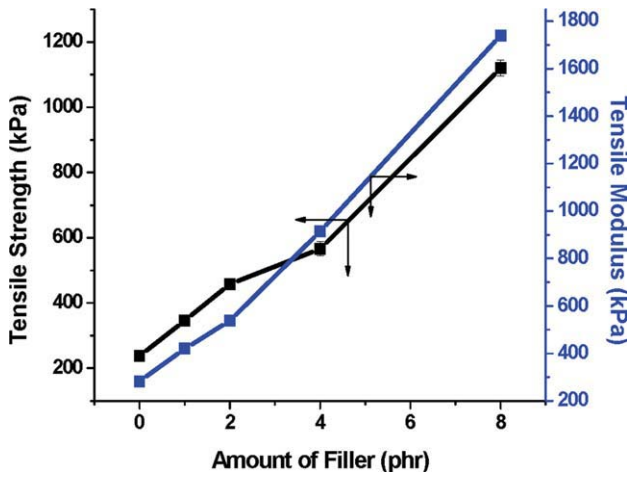

Figure 11 Plot of tensile strength and tensile modulus for *in situ* prepared amine modified CNF-hydroxyl PDMS nanocomposites as a function of filler loading. [Color figure can be viewed in the online issue, which is available at wileyonlinelibrary.com.]

TABLE V
Comparison of tan δ Results at T_g of Neat Rubber Vulcanizate and Its Nanocomposites

Sample	tan δ (T_g) (−116°C)
VP C0	0.195
VP C4	0.120
VP C8	0.109
PD C0	0.192
PD C4	0.174
PD C8	0.168
PD C4A	0.158
PD C8A	0.098

Effect of amine modification of CNF on mechanical properties for hydroxyl PDMS-based nanocomposites

Figure 11 shows a combined plot of tensile strength and tensile modulus with increasing filler concentration for *in situ* prepared amine modified CNF/hydroxyl PDMS nanocomposites. Mechanical properties thrive at their maximum for this filler–matrix combination since dispersion is improved by chemical functionalization. Furthermore, there is no side reaction analogous to that observed for vinyl terminated PDMS-based nanocomposites. Tensile strength is found to show an increase of 45, 92, 137, 370% while modulus increases by 48, 90, 223, 515% for 1, 2, 4, and 8 phr filler loadings respectively. Thus, chemical functionalization of filler is a way out for improving its state of dispersion in the polymer matrix which gets manifested in the upliftment of physico-mechanical properties of the nanocomposites.

Dynamic mechanical analysis

Representative results of dynamic mechanical analysis are compiled in Table V. Although there is no prominent shift in glass transition temperature (T_g) for the nanocomposites, there is a decent decrease in the height of the peak corresponding to the T_g (−116°C). This suggests that there is undoubtedly some interaction between polymer and filler. The decrease in height as well as slight broadening of the peak, which is more pronounced for nanocomposites with amine modified CNF, is an evidence for the greater extent of interaction between the polymer and the filler. Thus, from this observation it may be concluded that the amine groups introduced on the filler surface are contributing in an additional polymer–filler interaction, particularly H-bonding interaction as evident from the FTIR studies.

CONCLUSIONS

Novel CNF/PDMS nanocomposites were prepared by *in situ* polymerization and conventional *ex situ* solution casting method. Amine modification of CNF was carried out and nanocomposites were prepared with the same. A detailed scrutiny of the degree of dispersion of the nanofibers in the nanocomposites was done by analysis of the TEM images using image J software. *In situ* prepared nanocomposites showed better degree of filler dispersion as compared with the nanocomposites prepared by conventional methods. Extent of dispersion improved significantly by amine modification of filler. This was due to additional H-bonding interaction between the two phases. This type of interaction was evident from the ATR-FTIR studies which showed prominent shift in peak positions. The consequence of this interaction was evident from the increased crosslink density of the nanocomposites prepared with amine modified CNF-based PDMS nanocomposites. Increase in crosslink density was reflected in the improved mechanical properties of the nanocomposites. *In situ* amine modified CNF/vinyl PDMS nanocomposites showed only slight improvement in mechanical properties due to reduction in amount of hydride crosslinker by reaction with amine groups on the chemically modified filler. However, change in the matrix system yielded good results. For *in situ* prepared amine modified CNF/hydroxyl PDMS nanocomposites, tensile modulus increased by 515% while tensile strength showed an enhancement of 370% at 8 phr CNF loading. There was a prominent decrease in height of the peak corresponding to T_g thereby suggesting polymer–filler interaction. This nanocomposite also showed a decent increase of T_{max} by 114°C which was, however, less than the nanocomposite prepared with unmodified CNF (T_{max} increased by 141°C). This was due to the facilitated depolymerization of PDMS in presence of amine functionalities.

References

1. Faraz, M. I.; Bhowmik, S.; De Ruijter, C.; Laoutid, F.; Benedictus, R.; Dubois, P.; Page, J. V. S.; Jeson, S. J Appl Polym Sci 2010, 117, 2159.
2. Shi, Y.; Feng, X.; Wang, H.; Lu, X.; Shen, J. J Appl Polym Sci 2007, 104, 2430.
3. Niu, X.; Peng, S.; Liu, L.; Wen, W.; Sheng, P. Adv Mater 2007, 19, 2682.
4. Deng, H.; Bilotti, E.; Zhang, R.; Peijs, T. J Appl Polym Sci 2010, 118, 30.
5. Brown, G. M.; Ellyin, F. J Appl Polym Sci 2011, 119, 1459.
6. McDonald, J. C.; Whitesides, G. M. Acc Chem Res 2002, 35, 491.
7. Wang, K.; Li, W.; Gao;C. J Appl Polym Sci 2007, 105, 629.
8. Sun, Y. P.; Fu, K.; Lin, Y.; Huang, W. Acc Chem Res 2002, 35, 1096.
9. Niyogi, S.; Hamon, M. A.; Hu, H.; Zhao, B.; Bhowmik, P.; Sen, R.; Itkis, M. E.; Haddon, R. C. Acc Chem Res 2002, 35, 1105.
10. Blake, R.; Gunko, Y. K.; Coleman, J.; Cadek, M.; Fonseca, A.; Nagy, J. B.; Blau, W. J. J Am Chem Soc 2004, 126, 10226.
11. Tang, B. Z.; Xu, H. Y. Macromolecules 1999, 32, 2569.
12. Roy, N.; Bhowmick, A. K. Polymer 2010, 51, 5172.

13. Kuriger, R. J.; Alam, M. K.; Anderson, D. P.; Jacobsen, R. L. Compos Part A-Appl S 2002, 33, 53.
14. Finegan, I. C.; Tibbetts, G. G.; Gibson, R. F. Compos Sci Technol 2003, 63, 1629.
15. Cooper, C. A.; Ravich, D.; Lips, D.; Mayer, J.; Wagner, H. D. Comp Sci Technol 2002, 62, 1105.
16. Kumar, S.; Doshi, H.; Srinivasarao, M.; Park, J. O.; Schiraldi, D. A. Polymer 2002, 43, 1701.
17. Lozano, K.; Barrera, E. V. J Appl Polym Sci 2001, 79, 125.
18. Tibbetts, G. G.; McHugh, J. J. J Mater Res 1999, 14, 2871.
19. Ma, H.; Zeng, J.; Realff, M. L.; Kumar, S.; Schiraldi, D. A. Compos Sci Technol 2003, 63, 1617.
20. Takahashi, T.; Yonetake, K.; Koyama, K.; Kikuchi, T. Macromol Rapid Commun 2003, 24, 763.
21. Carneiro, O. S.; Covas, J. A.; Bernardo, C. A.; Caldeira, G.; Van Hattum, F. W. J.; Ting, J. M.; Alig, R. L.; Lake, M. L. Compos Sci Technol 1998, 58, 401.
22. Sandler, J.; Werner, P.; Shaffer, M. S. P.; Demchuk, V.; Altstadt, V.; Windle, A. H. Composite A 2002, 33, 1033.
23. Pogue, R. T.; Ye, J.; Klosterman, D. A.; Glass, A. S.; Chartoff, R. P. Compos Part A-Appl S 1998, 29, 1273.
24. Patton, R. D.; Pittman, C. U., Jr.; Wang, L.; Hill, J. R. Compos Part A-Appl S 1999, 30, 1081.
25. Dewimille, L.; Bresson, B.; Bokobza, L. Polymer 2005, 46, 4135.
26. McCarthy, D. W.; Mark, J. E.; Clarson, S. J.; Schaefer, D. W. J Polym Sci Part B Polym Phys 1998, 36, 1191.
27. Landry, C. J. T.; Coltrain, B. K.; Landry, M. R.; Fitzgerald, J. J.; Long, V. K. Macromolecules 1993, 26, 3702.
28. Sun, C. C.; Mark, J. E. Polymer 1989, 30, 104.
29. George, J. J.; Bhowmick, A. K. Nanoscale Res Lett 2008, 3, 508.
30. Bhowmick, A. K.; Hall, M. A.; Benarey, H. A. Rubber Products Manufacturing Technology; Marcel Dekker: New York, 1994, 317.
31. Flory, P. J.; Rehner, J. H. J Chem Phys 1943, 11, 521.
32. Pawlenko, S. Organosilicon Chemistry; Walter de Gruyter & Co.: Berlin, Germany; 1986.
33. Chalk, A. J.; Harrod, J. F. J Am Chem Soc 1965, 87, 16.
34. Luo, Z. P.; Koo, J. H. J Microsci 2007, 225, 118.
35. Oki, A.; Adams, L.; Khabashesku, V.; Edigin, Y.; Biney, P.; Luo, Z. P. Mater Lett 2008, 62, 918.
36. Socrates, G. Infrared Characteristic Group Frequencies; Wiley: Bristol; 1980, 126.
37. Arkles, B.C. US Patent 4,500,688, 1985.
38. Robertson, C. G.; Bogoslovov, R.; Ronald, C. M. Rubber Chem Technol 2009, 82, 202.
39. Xu, Y.; Higgins, B.; Brittain, W. J. Polymer 2005, 46, 799.
40. Camino, G.; Lomakin, S.; Lazzari, M. Polymer 2001, 42, 2395.
41. Lewicki, J. P.; Liggat, J. J.; Patel, M. Polym Degrad Stabil 2009, 94, 1548.
42. Fan, Y.; Lou, J.; Shinozaki, D. M. J Appl Polym Sci 2007, 103, 204.
43. Dalmas, F.; Chazeau, L.; Gauthier, C.; Cavaillé, J.-Y.; Dendievel, R. Polymer 2006, 47, 2802.
44. Bhattacharya, M.; Maiti, M.; Bhowmick, A. K. Polym Eng Sci 2009, 49, 81.
45. Bilotti, E.; Zhang, R.; Deng, H.; Quero, F.; Fischer, H. R.; Peijs, T. Compos Sci Technol 2009, 69, 2587.